Supporting Information

MAX-derived B-doped $Mo_{1.33}C$ MXene for ambient electrocatalytic nitrate to ammonia

Jianjia Mu, Da Wang, Shenye Zhou, Xianli Jia, Xuan-Wen Gao*, Zhaomeng Liu, Wen-Bin Luo*

Institute for Energy Electrochemistry and Urban Mines Metallurgy, School of Metallurgy,

Northeastern University, Shenyang, Liaoning 110819, China;

*) Corresponding address: gaoxuanwen@mail.neu.edu.cn; luowenbin@smm.neu.edu.cn

Experimental Section

Chemicals

Molybdenum powder (Aladdin, Mo, 99.99%), Yttrium powder (Aladdin, Y, 99.9%), Aluminum powder (Aladdin, Al, 99.95%), potassium nitrate ((Macklin, KNO_3, 99.5%), Hydrofluoric Acid (Macklin, NaOH, 40%), potassium hydroxide (Aladdin, KOH, AR), sodium hydroxide (Macklin, NaOH, AR), ammonium chloride (Macklin, NH_4Cl, 99%), sodium hypochlorite aqueous solution (Macklin, NaClO, CP), sodium citrate (Macklin, $C_6H_5Na_3O_7$, 98%), salicylic acid (Macklin, $C_7H_6O_3$, AR), sodium nitroprusside dihydrate (Macklin, $Na_2[Fe(CN)_5NO]\cdot 2H_2O$, AR), hydrazine hydrate (Aladdin, $N_2H_4\cdot H_2O$, 85%), Ultrahigh-purity N_2 (99.999%) and Ar (99.999%) were purchased from Shenyang Runqiao Gas Co., Ltd..

Synthesis of $(Mo_{2/3}Y_{1/3})_2AlC$ and $(Mo_{2/3}Y_{1/3})_2AlC_{0.9}B_{0.1}$

The raw materials were weighed following the stoichiometric ratio (Mo: Y: Al: C: B = 4: 2: 3.3: 2.7: 0.3), mechanically ball milled, and then compressed into pellets under an axial pressure of 100 MPa with a diameter of 16 mm. The as-prepared precursor was calculated at 1550 ℃ for 1 h with a heating rate of 10 ℃ min^{-1}. After cooling to room temperature, the target product $(Mo_{2/3}Y_{1/3})_2AlC_{0.9}B_{0.1}$ was obtained. For comparison, $(Mo_{2/3}Y_{1/3})_2AlC$ was prepared via similar procedures without boron powder addition.

Synthesis of $Mo_{1.33}C$ and $Mo_{1.33}C_{0.9}B_{0.1}$ MXene

Typically, 1g of the as-prepared powder was added into the hydrofluoric (HF) acid solution with a mass fraction of 40% under continuous magnetic stirring for 48 h at 35 ℃. After thorough etching, the as-obtained suspension was washed with 0.1 M HCl solution for three times and then washed with deoxygenated deionized water to make the suspension neutral accompanied by point probe sonication for 30 min at 400 W under an ice bath. The products were obtained by treating the as-sonicated suspension by lyophilization.

Material Characterization

The crystallographic arrangements of the specimens were assessed through X-ray powder diffraction technology (XRD). A field emission scanning electron microscope (SEM) was used to detect the micromorphologies of all samples. Transmission electron microscopy (TEM) equipped with an energy dispersive spectroscopy (EDS) detector was employed to acquire the nanoscale morphology and structural details. X-ray photoelectron spectroscopy (XPS, Thermo ESCALAB 250XI Al Kα X-ray source) was performed to detect the compositions and chemical state of as-synthesized materials.

Electrochemical Tests

Electrochemical measurement, in this work, was conducted with the DH7006 electrochemical workstation (Jiangsu Donghua) in a three-electrode system with a carbon paper (1.0 cm^2) loaded with 0.2 μg of electrocatalyst as working electrode, Hg/HgO electrode as the reference electrode, and Pt sheet as the counter electrode. H-type electrolysis cell was selected. The electrolyte was 1 M KOH aqueous solution containing 0.1 M KNO_3, and each of the cathode and anode chambers contained 50 mL of this solution. All potentials, in this paper, were expressed relatives to the reversible hydrogen electrode (RHE), which can be obtained through the equation below:

$$E_{RHE} = E_{Hg/HgO} + 0.098\ V + 0.0591 \times pH \quad (1)$$

Calculation of Ammonia Yield Rate and Faradic Efficiency

The ammonia yield rate was calculated via the indophenol blue method. Typically, 2 ml electrolyte after 2 h electrolysis was mixed with 1 M NaOH solution containing 5 wt.% (weight percentage) $C_7H_5O_3Na$ and 5 wt% $KNaC_4H_4O_6{\cdot}4H_2O$, and then accompanied by including 1 ml of NaClO aqueous solution (volume fraction of 6%) and 0.2 ml of 1wt.% $C_5H_4FeN_6Na_2O_3$ solution. Following a two-hour standing period, the yield rate was determined by the absorption peak intensity of the as-electrocatalyzed ammonia at 655 nm with a UV-vis spectrophotometer. Specifically, the NH_4^+ yield was calculated through the equation below:

$$Yield = \frac{c \times V}{t \times A} \quad (2)$$

in which c represents the concentration of as-synthesized NH_4^+, V is the electrolyte volume, t corresponds to the electrolysis time, and A is the geometric area of the working electrode.

The Faradic efficiency of ammonia production, in this work, was determined via the following equation:

$$FE = \frac{8F \times c \times V}{17Q} \quad (3)$$

where F and Q correspond to the Faradic constant and the entire amount of electric charge, respectively.

Calculation of Nitrite Yield Rate and Faradic Efficiency

0.10 mL of a 2.0 M HCl solution was added to 5 mL of diluted electrolyte in the test tubes. Then, 0.10 mL of N-(1-Naphthyl) ethylenediamine dihydrochloride solution at a concentration of 10 mg mL^{-1} was introduced into the mixture. After 30 minutes, the absorbance of NO_2^- was measured across the wavelength range from 650 nm to 450 nm. The final absorbance of NO_2^- was recorded at a wavelength of 540 nm. A standard calibration curve can be constructed using the specified concentrations of KNO_2 in a 1 M KOH solution.

DFT Calculation

In this work, density functional theory (DFT) calculations were conducted with the Vienna Ab initio Simulation Package (VASP)[1, 2]. The exchange-correlation was described using the Perdew-Burke-Ernzerhof (PBE) functional generalized gradient approximation (GGA). An energy cutoff of approximately 500 eV was selected for the plane wave kinetic energy, which was employed in the expansion of the wave functions for C, Mo, and B. The convergence criteria for total energy and force on each atom were set as 10^{-4} eV and 0.02 eV/Å, respectively. A model of a slab was constructed, incorporating a vacuum layer of 15 Å in the z-axis direction to mitigate interlayer interactions.

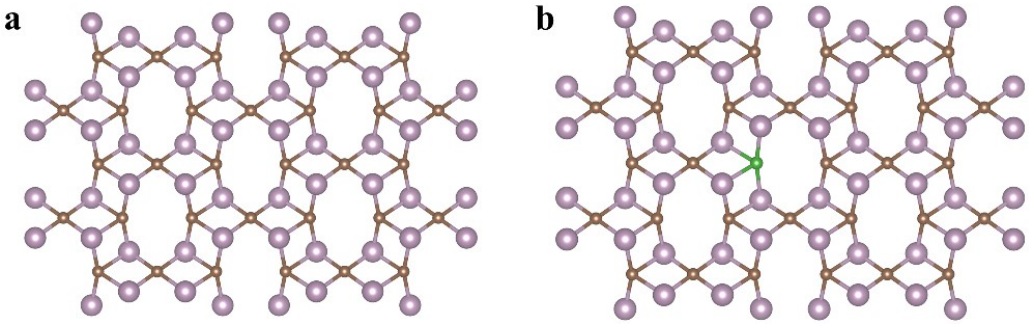

Fig. S1 The structure model of (a) $Mo_{1.33}C$ and (b) $Mo_{1.33}C_{0.9}B_{0.1}$.

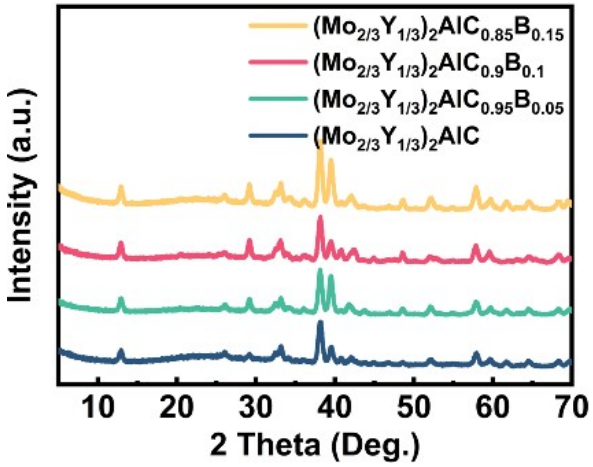

Fig. S2 XRD results of samples MAX with different content of B dopant.

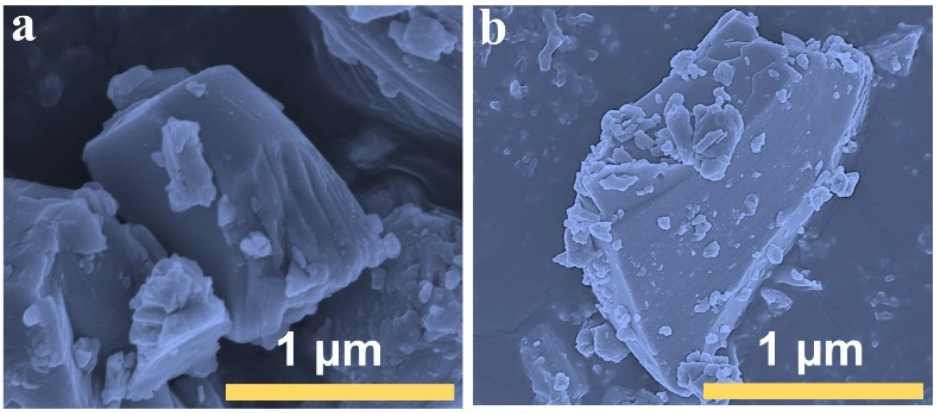

Fig. S3 SEM images of (a) $(Mo_{2/3}Y_{1/3})_2AlC$ and (b) $(Mo_{2/3}Y_{1/3})_2AlC_{0.9}B_{0.1}$.

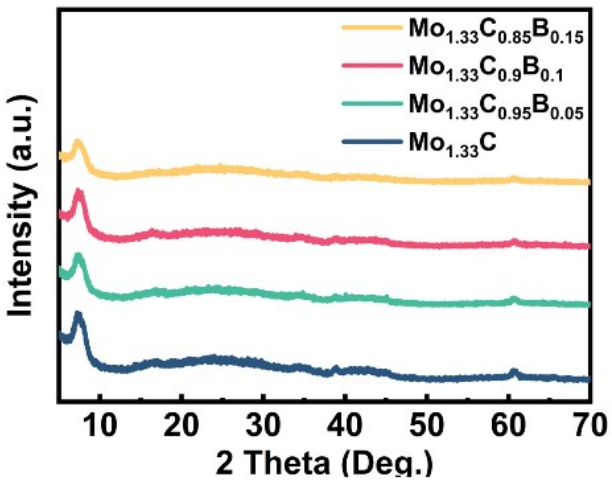

Fig. S4 XRD results of sample MXene with different content of B dopant.

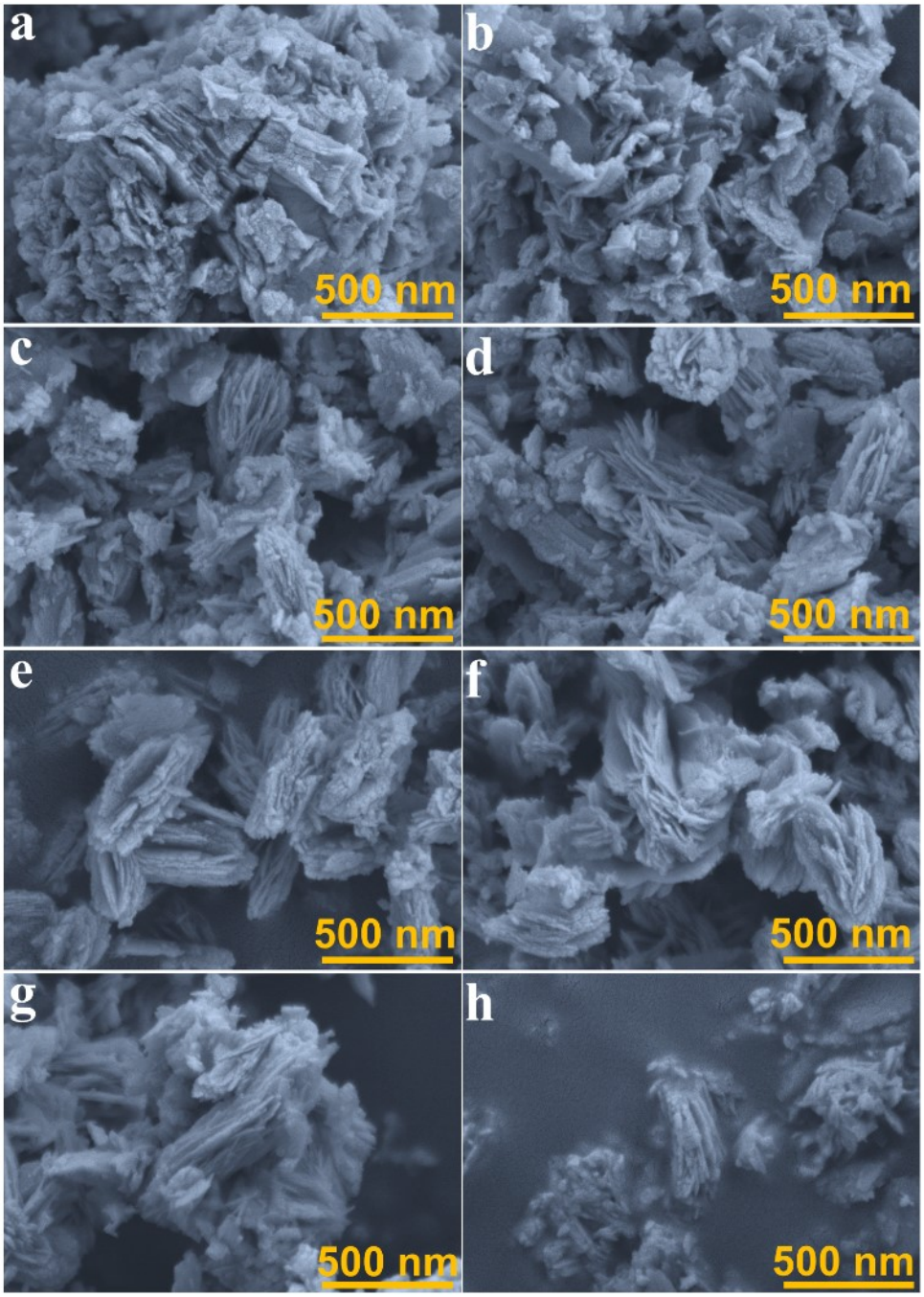

Fig. S5 SEM images of sample (a) $Mo_{1.33}C$, (b) $Mo_{1.33}C_{0.95}B_{0.05}$, (c) $Mo_{1.33}C_{0.9}B_{0.1}$, and (d) $Mo_{1.33}C_{0.85}B_{0.15}$.

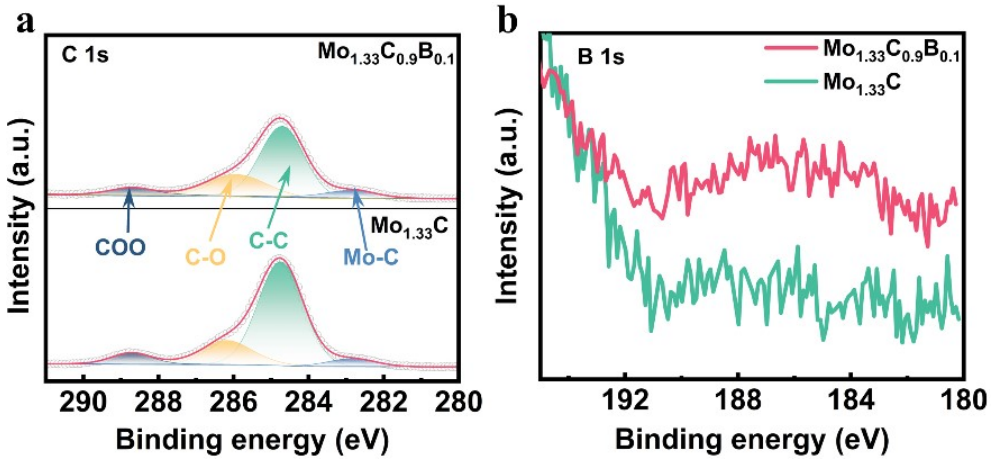

Fig. S6 High-resolution XPS spectra of (a) C 1s and (b) B1s from $Mo_{1.33}C$ and $Mo_{1.33}C_{0.9}B_{0.1}$.

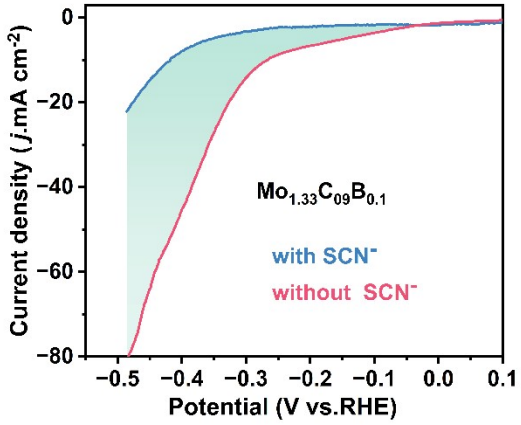

Fig. S7 LSV curves for poisoning experiment on $Mo_{1.33}C_{0.9}B_{0.1}$.

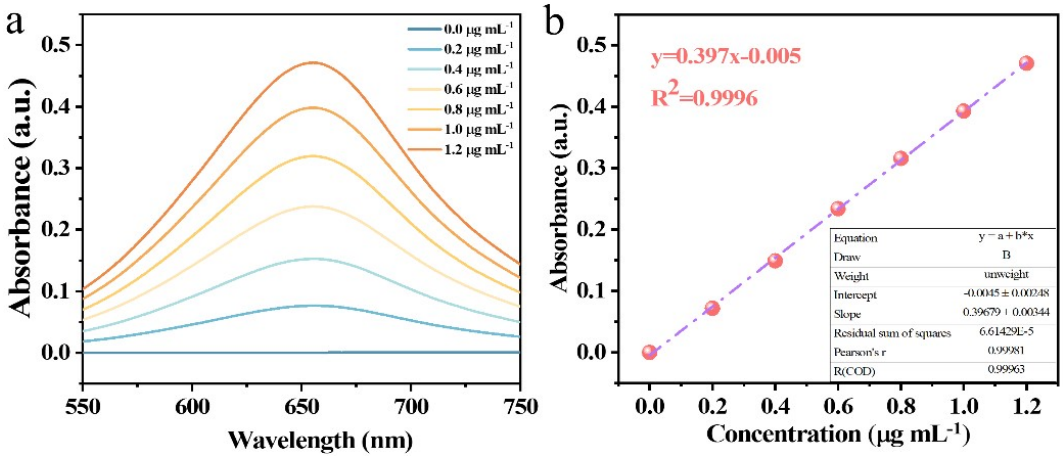

Fig. S8 (a) UV-Vis absorption spectra of standard ammonium chloride solution obtained by indophenol blue method in 1 M KOH after incubation for 2 h; (b) Calibration curve for estimating the NH_3 concentration.

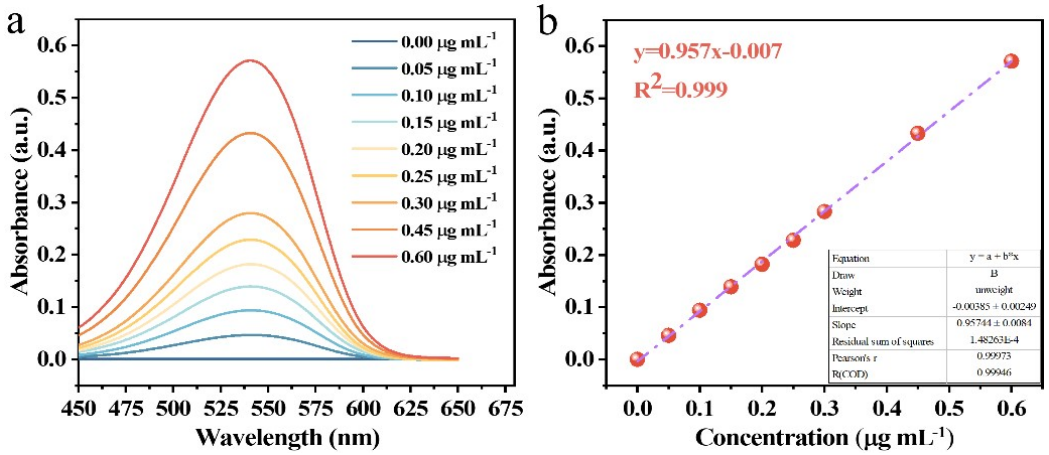

Fig. S9 (a) UV-Vis absorption spectra of standard KNO_2 solution in 1 M KOH after incubation for 30 min; (b) Calibration curve for estimating the NO_2^- concentration.

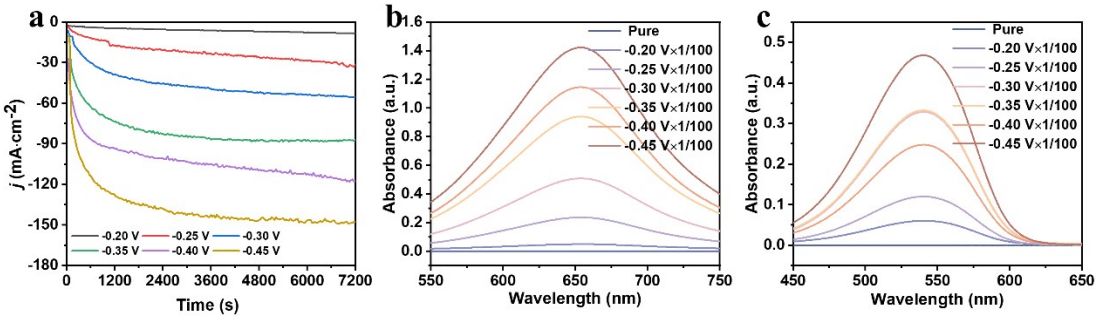

Fig. S10 NitRR performance of $Mo_{1.33}C_{0.9}B_{0.1}$ at different potentials. (a)Potential-dependent current density curves; UV-Vis absorption spectra of the electrolyte after 2h electrolysis for (b) NH_3 and (c) NO_2^-.

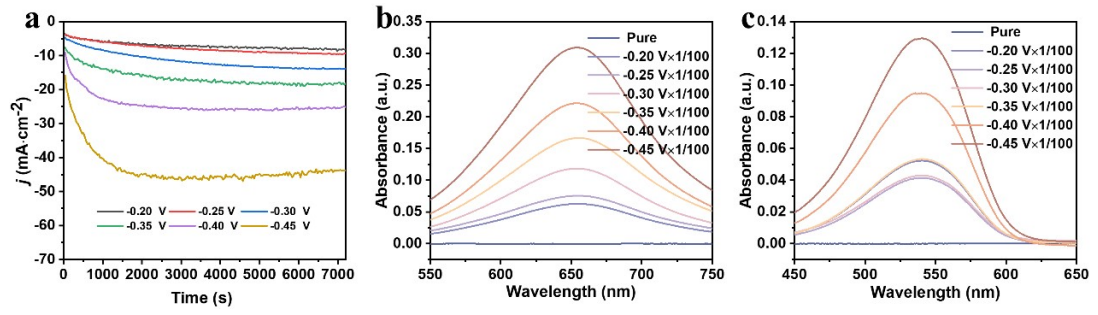

Fig. S11 NitRR performance of $Mo_{1.33}C$ at different potentials. (a) Potential-dependent current density curves; UV-Vis absorption spectra of the electrolyte after 2h electrolysis for (b) NH_3 and (c) NO_2^-.

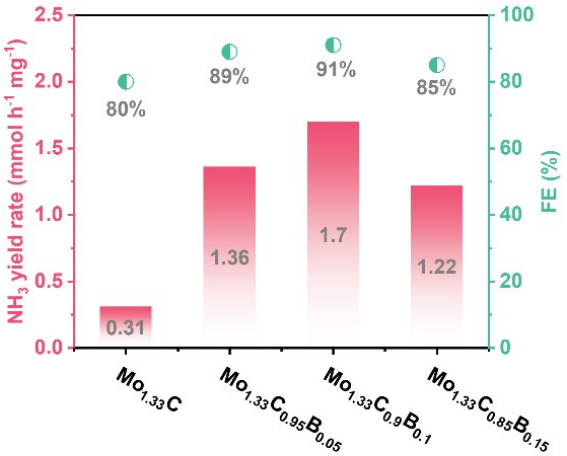

Fig. S12 The NH_3 yield rate and FE of all samples at -0.35 V.

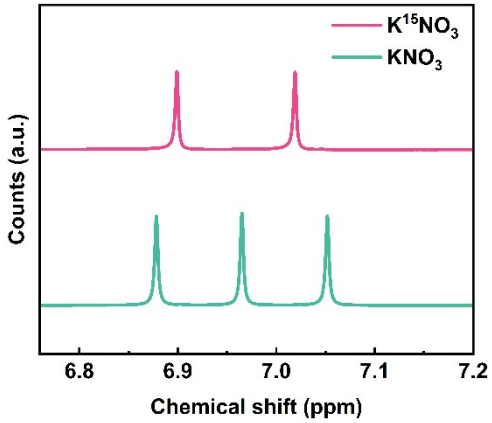

Fig. S13 ^1H nuclear magnetic resonance (NMR) spectra of the electrolyte with KNO_3 and $K_{15}NO_3$ after 2 h electrolysis on $Mo_{1.33}C_{0.9}B_{0.1}$ catalyst at -0.35 V.

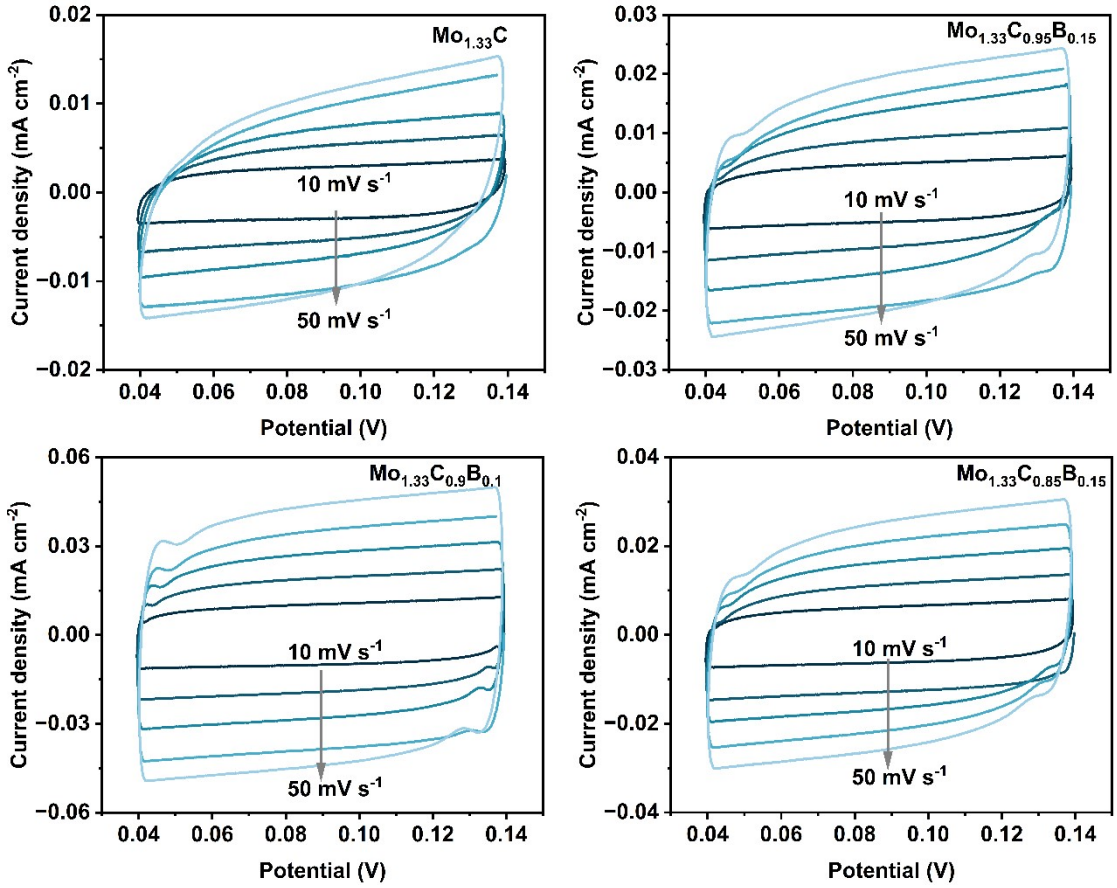

Fig. S14 CV tests from 0.04 to 0.14 V at various scan rates for evaluating the ECSA of as-prepared samples. (a) $Mo_{1.33}C$, (b) $Mo_{1.33}C_{0.95}B_{0.05}$, (c) $Mo_{1.33}C_{0.9}B_{0.1}$, and (d) $Mo_{1.33}C_{0.85}B_{0.15}$.

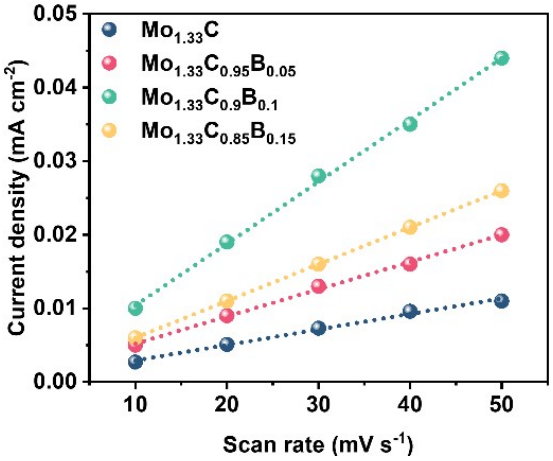

Fig. S15 Current density ($\Delta j = j_{anode} - j_{cathode}$) of different samples at 0.09 V plotted vs the scan rates.

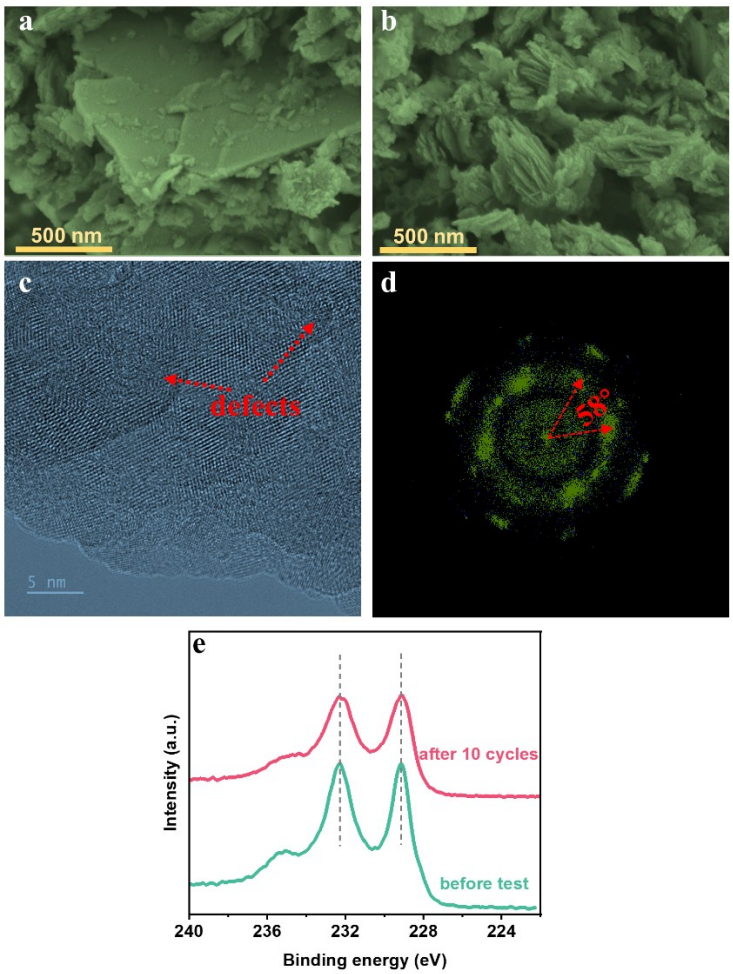

Fig. S16 (a, b) SEM images, (c) HRTEM, (d) SAED result of $Mo_{1.33}C_{0.9}B_{0.1}$ after cyclic tests, and (e) the high-resolution Mo XPS spectra of $Mo_{1.33}C_{0.9}B_{0.1}$ before and after cyclic tests.

Table S1 Comparison of the electrocatalytic NitRR performances of $Mo_{1.33}C_{0.9}B_{0.1}$ catalysts with other extensively reported electrocatalysts.

Catalysts	Potential (V vs. RHE)	NH_3 yield (mmol h^{-1} $mg_{cat.}^{-1}$)	Ref.
$Mo_{1.33}C_{0.9}B_{0.1}$	-0.35	1.7	This work
15%V–MoS_2	-1.2	0.014	*J. Mater. Chem. A*, 2022, 10, 23990–23997
10Cu/TiO_{2-x}	-0.75	0.1143	*J. Mater. Chem. A*, 2022, 10, 6448–6453
Cu_1Co_1–BCN	-0.5	0.38	***J. Mater. Chem. A***, 2023, **11**, 20234–20241
TiO_{2-x}	-0.94	0.045	*ACS Catal.*, 2020, 10, 6, 3533–3540
Cu/a-CeO_x	-0.5	1.52	*Adv. Energy Mater.* 2024, 14, 2303863
Fe_2TiO_5	-0.9	1.36	*Angew. Chem.Int. Ed.*, 2023, 135, e202215782

References

1. G. Kresse and J. Hafner, *Physical Review B*, 1993, 47, 558-561.
2. G. Kresse and J. Hafner, *Physical Review B*, 1994, 49, 14251-14269.